Breast Cancer: Targets and Therapy

Dovepress
Taylor & Francis Group

Open Access Full Text Article

ORIGINAL RESEARCH

The Prediction Model of High-Frequency Ultrasound Combined with Artificial Intelligence-Assisted Scoring System Improved the Diagnosis of Sclerosing Adenosis and Early Breast Cancer

Bingxin Ma[1], Gang Wu[1], Haohui Zhu[1], Yifei Liu[1], Wenjia Hu[1], Jing Zhao[1], Yinlong Liu[1], Qiuyu Liu[2]

[1]Department of Ultrasound, Henan Provincial People's Hospital, Zhengzhou, 450000, People's Republic of China; [2]Department of Pathology, Henan Provincial People's Hospital, Zhengzhou, 450000, People's Republic of China

Correspondence: Gang Wu, Email drwugang325@126.com; Haohui Zhu, Email zhh761126@163.com

Objective: The study aimed to apply an artificial intelligence (AI)-assisted scoring system, and improve the diagnostic efficiency of Sclerosing adenosis and early breast cancer.

Methods: This study retrospectively collected adenopathy patients (156 cases) and early breast cancer patients (150 cases) in Henan Provincial People's Hospital from August 2020 to April 2023.

Results: The area under the curve of the model constructed by clinical ultrasound features and combined AI features to predict and identify the two in the training group was 0.89 and 0.94, respectively. The combined AI model with the best performance (training AUC, 0.94, 95% CI, 0.91–0.97 and validation AUC, 0.95, 95% CI, 0.90–0.99) was superior to the clinical ultrasound feature model, and the decision curve also showed that the clinical ultrasound combined with AI Nomogram had good clinical practicability. In the training group, the AUC of the sonographer and AI in differential diagnosis was 0.67(95% CI, 0.62–0.71) and 0.89(95% CI, 0.84–0.93), respectively, and the sonographer's assessment showed better sensitivity (1.00 VS 0.73), but AI showed a higher accuracy rate (0.66 VS 0.80).

Conclusion: Age, lesion size, burr, blood flow, and AI risk score are independent predictors of sclerosing adenosis and early breast cancer. The combined clinical ultrasound feature and AI model are correlated with AI risk score, US routine features, and clinical data, superior to the clinical ultrasound model and BI-RADS grading, and have good diagnostic performance, which can provide clinicians with a more effective diagnostic tool.

Keywords: sclerosing adenosis, breast tumor, ultrasound, AI, computer-aided diagnosis

Introduction

Sclerosing adenosis (SA), is a benign but complex hyperplastic lesion. Among the benign lesions undergoing biopsy, the incidence of SA is about 27.8%.[1] Pathologically, it is often accompanied by interstitial and acinar hyperplasia, resulting in different degrees of lobular extrusion and distortion.[2] Due to its pathological growth characteristics, SA presents an aggressive appearance and is often combined with other lesions, and its imaging manifestations are complex and diverse, making it extremely difficult to distinguish from malignant breast lesions.[3] Histopathological examination is the gold standard for the diagnosis of SA.[4,5] Although some studies believe that SA as a single feature will approximately double the risk of breast cancer,[1] surgical resection is not necessary when SA is present alone in biopsy.[6] The clinical treatment recommendation is a close clinical follow-up or routine review, which avoids unnecessary surgical biopsy for patients and guides clinicians to make accurate decisions. Therefore, preoperative noninvasive evaluation is crucial.

Received: 19 June 2024
Accepted: 16 January 2025
Published: 7 February 2025

With the continuous progress of medical imaging technology and computer technology, it is possible to use computer software to extract information that is difficult to identify by the naked eye from medical images, because it can automatically identify image information for quantitative evaluation of lesions, and has been increasingly applied to breast ultrasound.[7,8] The application of computer software not only saves the examination time for ultrasound doctors but also makes up for some of the shortcomings of beginners' experience and skills. Therefore, computer-aided diagnosis is expected to become a powerful tool to help doctors carry out clinical diagnosis. Current studies suggest that SA has mostly asymptomatic clinical manifestations, is difficult to find out during physical examination, and the lesions are small, with the maximum diameter of the lesions mostly less than 2 cm.[9] However, when the lesions of breast cancer are larger, the corresponding malignant signs are more obvious, and the differentiation of large nodules between the two has little influence on preoperative evaluation and clinical treatment decisions. The difficulty of differentiation lies in SA and early breast cancer (T1 stage). At present, most scholars focus on the differentiation between SA and early breast cancer, and there is no further stratified analysis of nodule size. There is no systematic study on whether an AI-assisted scoring system can distinguish between SA and early breast cancer, and whether combining conventional US features, elastic imaging techniques, and clinical data can improve the predictive value of distinguishing between the two. Therefore, the purpose of this study is to evaluate the practical value of an AI-assisted scoring system in distinguishing the SA and early breast cancer, establish and evaluate the usefulness of the Nomogram model, and provide references for sonographers to solve the problems in their work.

Methods and Materials

Subject

A retrospective analysis was performed on 504 patients with SA and breast cancer confirmed by surgery and pathology in Henan Provincial People's Hospital from August 2020 to April 2023. Inclusion criteria: Clinically suspected malignant breast lesions or benign nodules with a high probability that the patient strongly requested surgery; Ultrasound and elastography were used for biopsy or preoperative evaluation, accompanied by examination with an AI-assisted scoring system; The maximum diameter of the lesion was less than 2 cm, which was pathologically confirmed as early breast cancer,[10] and no metastasis or distant metastasis was found in ipsilateral axillary lymph nodes. Exclusion criteria: Conventional ultrasound, elastic characteristics, or AI information is incomplete; No nodules were found in imaging, but punctate or focal SA was inadvertently discovered in pathology; Conventional ultrasound lesions were more than 2 cm or multifocal lesions; The pathology confirmed SA with malignant lesions. Finally, 306 patients were included in this study and were randomly divided into a training group (n = 214) and a validation group (n = 92). The study flow chart is summarized in Figure 1. The study was retrospective; thus, the ethical examination was approved by the Henan People's Hospital Committee and informed consent was acquired.

Instruments

Ultrasonic examination: Germany Siemens Sequoia color Doppler ultrasonic diagnostic instrument, 9L4 linear array probe, frequency 5.0–14.0 MHz was used. Routine breast ultrasound is performed by an ultrasound doctor with more than 10 years of experience, and ultrasonic characteristics are recorded when lesions are found. Including lesion location, size, shape (oval or round, irregular), edge (clear, fuzzy), burr (yes, no), growth direction (parallel, no parallel), internal echo (low echo, high echo, mixed echo), calcification (yes, no), rear echo characteristics (enhanced, no echo, attenuation) and blood supply (yes, no), etc. According to the 5th edition[11] "Breast Imaging Reporting and Data System" (BI-RADS) of the American College of Radiology, breast masses were interpreted, and the classification results were evaluated by a dichotomy: BI-RADS 3 was "probably benign"; BI-RADS 4a and above are "possibly malignant". When the grayscale image was clear and stable, it was switched to EI mode to obtain a satisfactory elastic image, and an elastic strain rate ratio (SR) measurement was performed. Measurement methods: Area of interest A was obtained at the edge of the outline lesion, and area of interest B was obtained at the same depth of glandular tissue. The strain rate ratio (B/A) was automatically obtained by the machine, and the average value was obtained after 3 consecutive measurements. AI-assisted diagnostic system measurement: AI-SONICTM series auxiliary breast diagnosis system (Zhejiang Desang

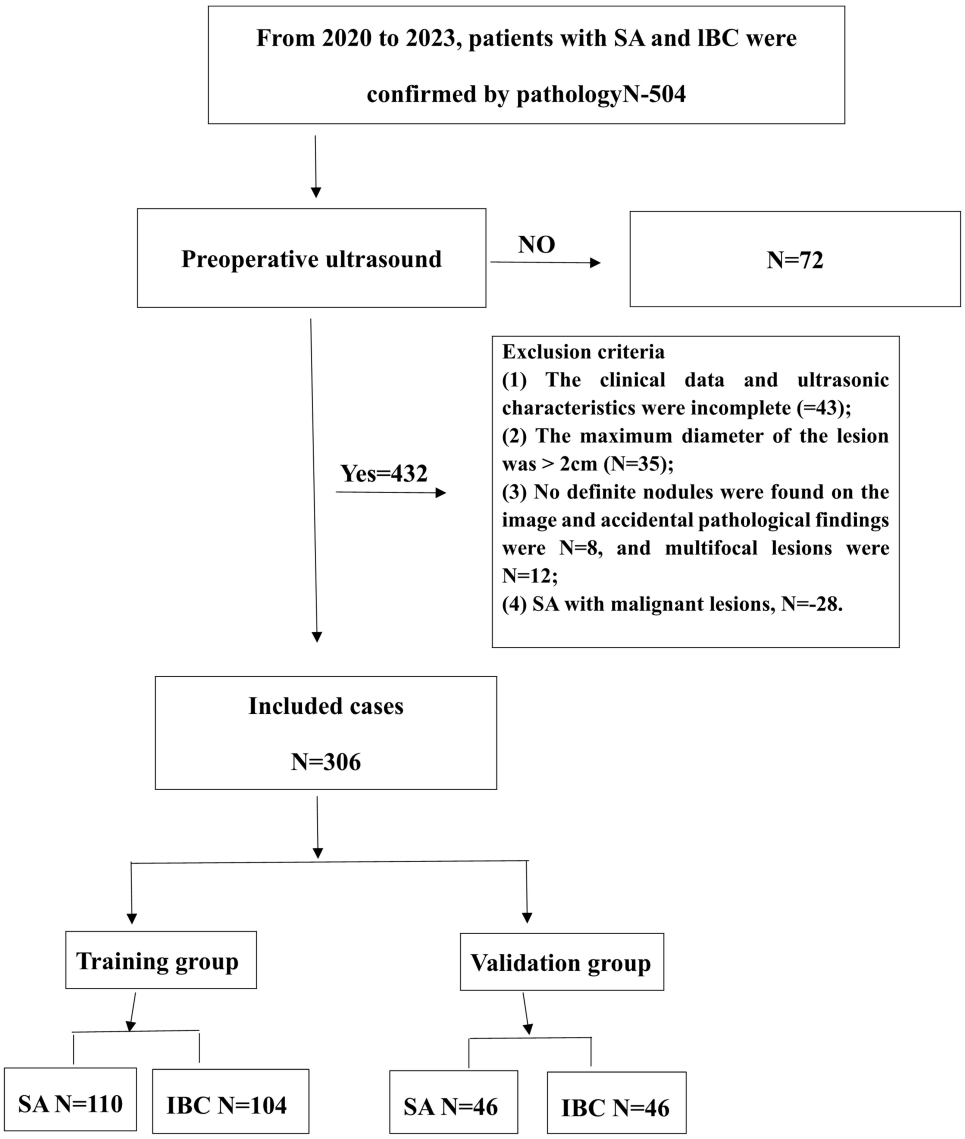

Figure 1 Flow chart.
Abbreviations: SA, Sclerosing adenosis; IBC, Invasive breast carcinoma.

Yunxing Medical Technology) was used for examination. According to the terms of service and contract, using the AI platform to write this article is permitted. This system uses a DE-light deep learning technology platform to train a large number of ultrasound images of breast lesions and develops an intelligent breast auxiliary diagnosis system with high accuracy and rapidity.

The inspection operation is carried out synchronously and in real-time with conventional ultrasound. In the early stage, an application engineer of an AI Automatic Detection System company provides standardized supervision and guidance to the operator in the whole process, to facilitate the acquisition of the best standardized ultrasound section image. Images are transmitted synchronously to the auxiliary diagnostic system server during the doctor's scan, and the image is frozen when the best standard ultrasound image is obtained. The auxiliary system displays the nodule on the same screen and carries out automatic labeling, processing, and analyzing. Each nodule is displayed in vertical and transverse sections twice, frozen in real time, stored, and transmitted to the automatic interpretation system. AI algorithm automatically quantifies the 5 characteristics of breast nodules, such as size, boundary, shape, internal echo, and calcification focus. When the BI-RADS classification and risk probability value tend to be stable, the recording system automatically interprets the highest BI-RADS classification and AI risk score of nodules.[12]

https://doi.org/10.2147/BCTT.S483496

Model Construction

The predictive model was constructed based on the training group. The steps were as follows: First, possible predictors of outcome events were screened out based on single-factor logistic regression analysis ($P<0.05$). For the selected variables, the LASSO logistic regression algorithm is used to select significant features (coefficients are non-zero). The optimal parameter configuration was determined using 10-fold cross-validation, and coefficients were determined based on the lambda value corresponding to the minimum distance deviation and a standard error, and variables with non-zero coefficients were screened out. For the selected variables, multivariate logistic regression analysis (stepwise, two-way) was carried out. The prediction model nomogram was constructed based on the variables $P<0.05$ in the stepwise method, and 1000 bootstrap samples were sampled for validation. Calibration curves were drawn to evaluate the calibration degree of the model. Further, AUC, sensitivity, specificity, accuracy, and other indexes were calculated through receiver operating characteristic (ROC) curve analysis to evaluate its discrimination efficiency. DCA was constructed to evaluate the clinical application value of the model, and finally, the constructed model was validated in the validation set.

Statistical Method

R language statistical software (version 4.3.1) and MSTATA software package were used to process and analyze the data. Continuous variables, if they conform to a normal distribution, are described statistically with mean ± standard deviation. Independent sample *t*-test was used for comparison between groups. If the distribution does not conform to normal, the median [P25, P75] is used to describe the distribution. The rank sum test was used for comparison between groups. Counting data were described by case number (%), and the Chi-square test was used for comparison between groups. The "rms" package was used to draw Nomogram construction and calibration. The "ggDCA" package is used for clinical decision curve analysis. A bilateral test $P<0.05$ was considered statistically significant.

Results

Comparison of Clinical Data, Ultrasound Characteristics, Elastic Characteristics, and AI Characteristics Between the Training Group and the Validating Group

All the patients were female, with a total of 306 cases. Pathologically confirmed, of the 156 SA cases, 75 were simple SA, 30 were combined with fibroadenoma, 26 were combined with atypical hyperplasia, and 25 were combined with intraductal papilloma. Among 150 cases of early breast cancer, 124 were invasive ductal carcinoma, 18 were invasive lobular carcinoma, and 8 were tubular carcinoma. Clinical parameters include Age, Menopause, Family history of breast cancer; Ultrasonic characteristic parameters include Lesion size, Margin, Morphology, Lobulation, Burr, Echo, Calcification, Posterior Echo, Blood supply, Aspect Ratio, Elastic Strain Rate. AI parameters include AI risk score.

The results showed that there was no significant difference between the training group and the validation group in lesion size, age, menstrual history, family history, other ultrasound features, elastic information, and AI features (p= 0.204–1.000), except for calcification (p=0.009, Table 1).

Training Group Baseline Data, Univariate and Multivariate Analysis

Univariate analysis in the training group, age, menopausal history, tumor size, boundary, presence or absence of burrs, rear echo attenuation, blood supply, elastic strain rate ratio, and AI risk score were statistically significant (Table 2). Variables with P<0.05 in the single factor were included in the lasso regression analysis (Figure 2a and b). Based on the minimum deviation from a standard error corresponding to a lambda value (0.0389), the screening coefficient is a variable with non-zero. In multivariate logistic regression analysis, age, size, burr or not, blood supply, and AI risk score were finally selected as potential risk factors to predict and used for the construction of the prediction model's nomogram (Table 3 and Figure 3a).

Construction and Verification of Clinical Ultrasound Model and Clinical Ultrasound-AI Combined Model

The AUC of the clinical ultrasound model was established according to patient clinical data and ultrasound characteristics and combined AI information was 0.89 (95% CI: 0.84–0.93) and 0.94 (95% CI: 0.91–0.97), respectively. The

Table 1 Characteristics Between the Training Group and the Validating Group

	ALL N=306 M (P25, P75)/N (%)	**Training N=214 M (P25, P75)/N (%)**	**Validating N=92 M (P25, P75)/N (%)**	**p. overall**
Age	46.50 [42.00; 52.00]	47.00 [43.00; 52.00]	46.00 [40.00; 51.00]	0.204
Menopause:				0.574
No	194 (63.40%)	133 (62.15%)	61 (66.30%)	
Yes	112 (36.60%)	81 (37.85%)	31 (33.70%)	
Family_history_of_breast_cancer:				0.118
No	293 (95.75%)	202 (94.39%)	91 (98.91%)	
Yes	13 (4.25%)	12 (5.61%)	1 (1.09%)	
Lesion_size (mm)	12.00 [10.00; 16.00]	12.00 [9.00; 16.00]	12.00 [10.00; 15.25]	0.795
Margin				0.920
Clear	229 (74.84%)	161 (75.23%)	68 (73.91%)	
Unclear	77 (25.16%)	53 (24.77%)	24 (26.09%)	
Morphology:				1.000
Regular	99 (32.35%)	69 (32.24%)	30 (32.61%)	
Irregular	207 (67.65%)	145 (67.76%)	62 (67.39%)	
Lobulation:				0.717
Yes	186 (60.78%)	132 (61.68%)	54 (58.70%)	
No	120 (39.22%)	82 (38.32%)	38 (41.30%)	
Burr:				0.800
No	138 (45.10%)	95 (44.39%)	43 (46.74%)	
Yes	168 (54.90%)	119 (55.61%)	49 (53.26%)	
Echo:				0.577
Hypoecho	290 (94.77%)	204 (95.33%)	86 (93.48%)	
Mixed echo	16 (5.23%)	10 (4.67%)	6 (6.52%)	
Calcification:				0.009
No	234 (76.47%)	173 (80.84%)	61 (66.30%)	
Yes	72 (23.53%)	41 (19.16%)	31 (33.70%)	
Posterior_Echo:				0.307
Unchanged	236 (77.12%)	165 (77.10%)	71 (77.17%)	
Enhanced	46 (15.03%)	35 (16.36%)	11 (11.96%)	
Damped	24 (7.84%)	14 (6.54%)	10 (10.87%)	
Blood_supply:				0.281
Unabundant	208 (67.97%)	150 (70.09%)	58 (63.04%)	
Abundant	98 (32.03%)	64 (29.91%)	34 (36.96%)	
Aspect_Ratio:				1.000
Horizontal growth	212 (69.28%)	148 (69.16%)	64 (69.57%)	
Vertical growth	94 (30.72%)	66 (30.84%)	28 (30.43%)	
Elastic_Strain_Rate	4.20 [3.20; 6.27]	4.20 [3.20; 6.27]	4.15 [3.18; 6.23]	0.633
AI_risk score	0.58±0.27	0.59±0.27	0.56±0.27	0.340

Table 2 Comparison of Baseline Data of SA and Breast Cancer in the Training Group

	SA N=110	**IBC (Invasive Breast Carcinoma) N=104**	**p**
Age	44 [40.00; 48.75]	49 [45.00; 58.00]	<0.001
Menopause:			0.002
No	80 (72.73%)	53 (50.96%)	
Yes	30 (27.27%)	51 (49.04%)	

(*Continued*)

https://doi.org/10.2147/BCTT.S483496

Table 2 (Continued).

	SA N=110	**IBC (Invasive Breast Carcinoma) N=104**	**p**
Family_history_of_breast_cancer:			0.321
No	106 (96.36%)	96 (92.31%)	
Yes	4 (3.64%)	8 (7.69%)	
Lesion_size(mm)	11.00 [8.00; 14.75]	14.00 [12.00; 17.00]	<0.001
Margin:			<0.001
Clear	103 (93.64%)	58 (55.77%)	
Unclear	7 (6.36%)	46 (44.23%)	
Morphology:			0.777
Regular	34 (30.91%)	35 (33.65%)	
Irregular	76 (69.09%)	69 (66.35%)	
Lobulation:			0.921
No	67 (60.91%)	65 (62.50%)	
Yes	43 (39.09%)	39 (37.50%)	
Burr:			<0.001
No	71 (64.55%)	24 (23.08%)	
Yes	39 (35.45%)	80 (76.92%)	
Echo:			1.000
Hypoecho	105 (95.45%)	99 (95.19%)	
Mixed echo	5 (4.55%)	5 (4.81%)	
Calcification:			0.112
No	94 (85.45%)	79 (75.96%)	
Yes	16 (14.55%)	25 (24.04%)	
Posterior_Echo:			<0.001
Unchanged	98 (89.09%)	67 (64.42%)	
Enhanced	7 (6.36%)	28 (26.92%)	
Damped	5 (4.55%)	9 (8.65%)	
Blood_supply:			<0.001
Unabundant	93 (84.55%)	57 (54.81%)	
Abundant	17 (15.45%)	47 (45.19%)	
Aspect_Ratio:			0.900
Horizontal growth	77 (70.00%)	71 (68.27%)	
Vertical growth	33 (30.00%)	33 (31.73%)	
Elastic_Strain_Rate	3.60 [2.80; 4.50]	4.85 [4.00; 7.65]	<0.001
AI_risk score	0.419±0.260	0.780±0.115	<0.001

calibration curve is close to the ideal diagonal (Figure 3b). Compared with BI-RADS grading and clinical ultrasound models, the combined AI model showed higher diagnostic efficiency in ROC analysis (Figure 3c and d). By comparing the models, the combined model showed the best performance and the best AUC value in the training group (0.94; 95% CI: 0.91–0.97). The AUC for sonographers and AI was 0.67 (95% CI: 0.63, 0.72) and 0.89 (95% CI: 0.85, 0.93) (Figure 3c). Therefore, clinical ultrasound features combined with the AI model have a satisfactory ability to distinguish SA and early IBC. The AI model combining all features showed a relatively better specificity of 0.92 (95% CI: 0.87, 0.97) and diagnostic accuracy of 0.90 (95% CI: 0.90, 0.90) than the other models (Table 4). The sonographer's assessment accuracy was lower by 0.66 (95% CI: 0.66, 0.67), but showed better sensitivity (1.00 (95% CI: 1.0–1.0) (Table 4).

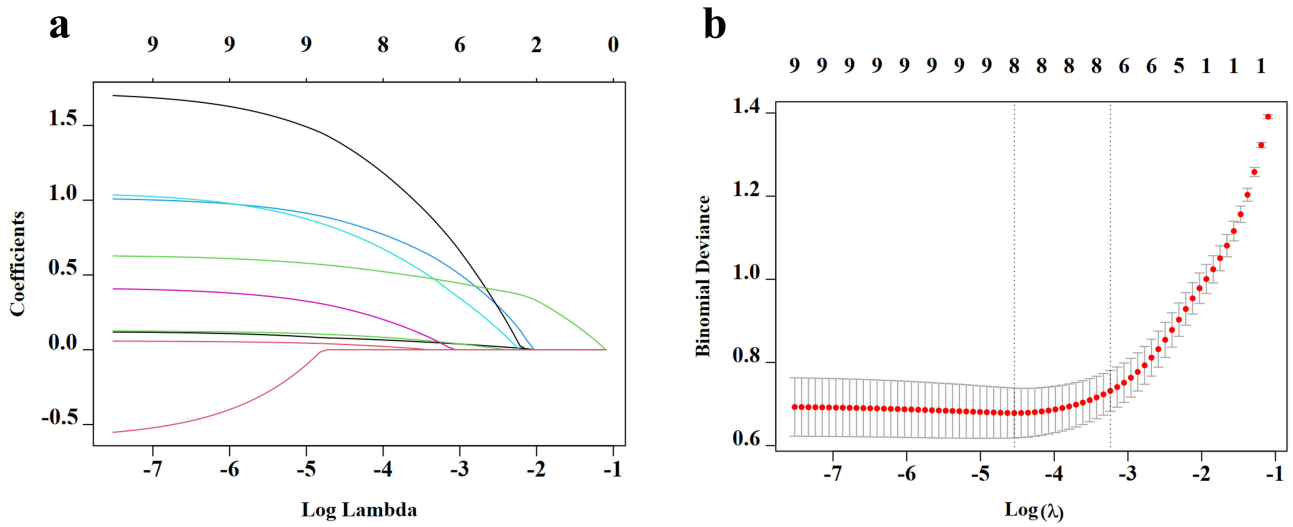

Figure 2 In the LASSO binary logistic regression model, the parametric algorithm was used to select the radiomic features. (**a**) The Lasso coefficient, the adjustment parameter (λ) in the LASSO model is selected using the ten-fold cross-validation via the minimum criterion. (**b**) Ten-fold cross-verify the production coefficient plot with the selected log λ value.

Discussion

In our study, we combined clinical data, ultrasound features, and AI information to develop a nomogram for the differential diagnosis of SA and early IBC, which demonstrated better diagnostic efficacy and clinical practicality. SA is a common proliferative disease and was present in 62.4% of biopsies with hyperplastic disease and 55.1% of biopsies

Table 3 Univariate and Multivariate Analysis in the Training Group

Variable	Univariate Analysis OR (95% CI) P	Multivariate Analysis OR (95% CI) P
Age	1.103 (1.065, 1.147) <0.001	1.106(1.049, 1.176) <0.001
Menopause		
No	Reference	
Yes	2.566 (1.461, 4.571) 0.001	NA
Family_history_of_breast_cancer		
No	Reference	
Yes	2.208 (0.673, 8.489) 0.207	NA
Lesion_size	1.163 (1.087, 1.249) <0.001	1.137 (1.018, 1.277) 0.025
Margin		
Clear	Reference	
Unclear	11.670 (5.241, 29.817) <0.001	2.890 (0.954, 9.773) 0.070
Morphology		
Regular	Reference	
Irregular	0.882 (0.496, 1.566) 0.668	NA
Lobulation		
No	Reference	
Yes	0.935 (0.538, 1.623) 0.811	NA
Burr		
No	Reference	
Ye	6.068 (3.371, 11.235) <0.001	2.778 (1.098, 7.278) 0.033
Echo		
Hypoecho	Reference	
Mixed echo	1.061 (0.287, 3.920) 0.928	NA

(*Continued*)

https://doi.org/10.2147/BCTT.S483496

Table 3 (Continued).

Variable	Univariate Analysis OR (95% CI) P	Multivariate Analysis OR (95% CI) P
Calcification		
No	Reference	
Yes	1.859 (0.935, 3.787) 0.080	NA
Posterior_Echo		
Unchanged	Reference	
Enhanced	5.851 (2.539, 15.259) <0.001	NA
Damped	2.633 (0.870, 8.891) 0.095	NA
Blood_supply		
Unabundant	Reference	
Abundant	4.511 (2.405, 8.790) <0.001	6.376 (2.364, 19.278) <0.001
Aspect_Ratio		
Horizontal growth	Reference	
Vertical growth	1.085 (0.606, 1.941) 0.784	NA
Elastic_Strain_Rate	1.243 (1.120, 1.396) <0.001	NA
AI_risk score	2.413 (1.918, 3.241) <0.001	1.941 (1.526, 2.633) <0.001

Abbreviations: CI, confidence interval; OR, odds ratio; ref, reference. CI.

with atypical hyperplasia in the Mayo Benign Breast Disease cohort. In this study, the nomogram predicted that 50% of the screened patients in the relevant population would develop sclerotic adenopathy, which was consistent with the report of Visscher et al.[1] SA is a non-neoplastic benign epithelial hyperplastic lesion,[13] often accompanied by other hyperplastic

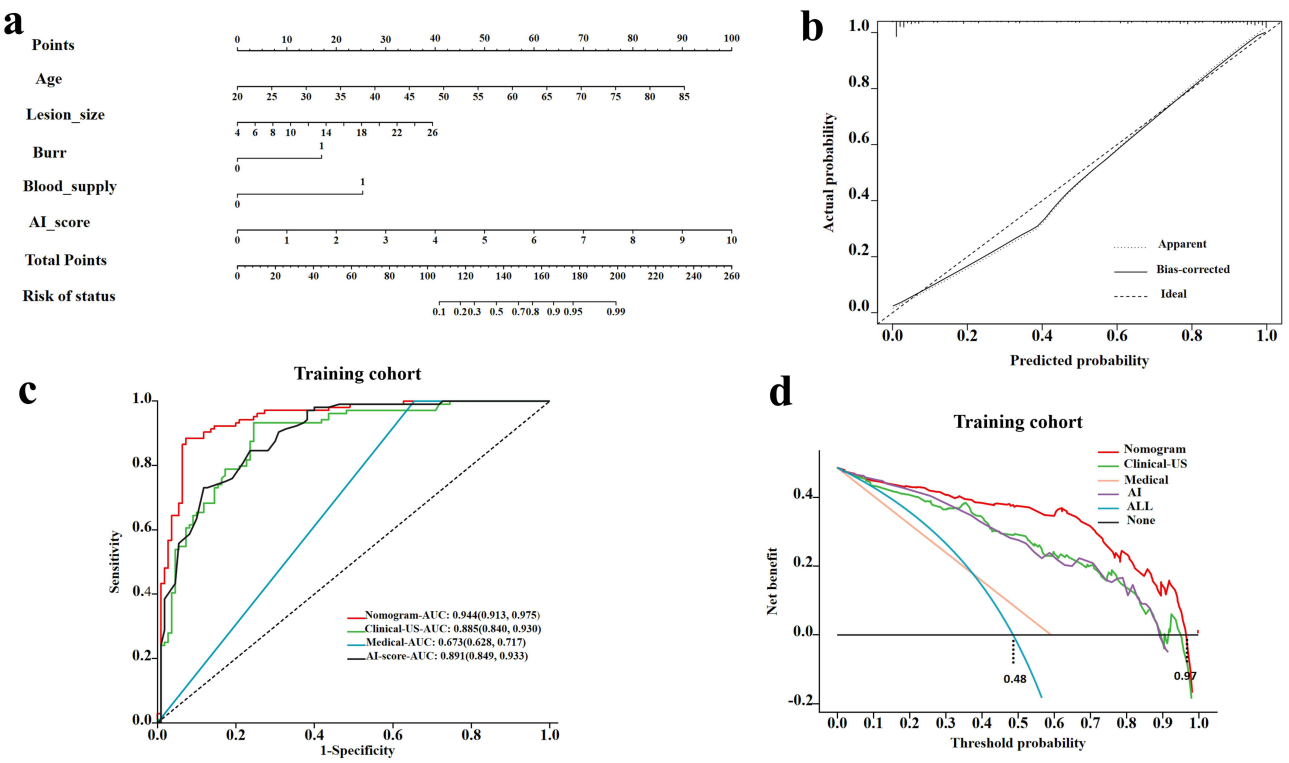

Figure 3 (**a**) Combined nomogram constructed from clinical features, ultrasound features, and AI risk score, with predictors including age, tumor size, presence or absence of burrs, blood supply, and AI risk score; (**b**) In the calibration curve, the horizontal coordinate represents the probability predicted by Nomogram, and the vertical coordinate represents the actual probability of malignant lesions. Bias correction was performed through 1000 bootstrap sample sampling validation to evaluate the model calibration degree and Nomogram performance. (**c**) Nomogram AUC curve (red) contains variables such as Age, lesion size, burr, blood flow, and AI risk score. Clinical-US-AUC curve (green) contains variables such as age, menopause, lesion size, Burr, blood flow. Medical-AUC curve (blue) contains variables classified by the ultrasound doctor BI-RADS. Ai-score-AUC curve (black) variable is AI risk score. (**d**) The threshold probability corresponds to the horizontal coordinate of the DCA curve. The benefit of the model "all" line can be obtained by drawing a vertical line, while the benefit of "none" line is zero. The threshold of the training set ranges from 0 to 0.97, and all the nomogram show the benefit.

Table 4 Analysis and Comparison of Combined AI Model With Clinical Ultrasound Characteristic Model, Physician BI-RADS, and AI-BI-RADS

Character	AUC	Sensitivity	Specificity	Accuracy
Joint AI model	0.94(0.91, 0.97)	0.88(0.82, 0.94)	0.92(0.87, 0.97)	0.90(0.90, 0.90)
Clinical ultrasound characteristic model	0.89(0.84, 0.93)	0.93(0.88, 0.98)	0.75(0.67, 0.83)	0.84(0.84, 0.84)
Sonographer BI-RADS grading	0.67(0.63, 0.72)	1.00(1.00, 1.00)	0.34(0.25, 0.43)	0.66(0.66, 0.67)
AI-BI-RADS grading	0.89(0.85, 0.93)	0.73(0.64, 0.81)	0.88(0.82, 0.94)	0.80(0.80, 0.81)

Notes: The Joint AI model contains variables age, lesion size, burr, blood flow, and AI risk score. Clinical ultrasound characteristic model parameters include age, menopause, lesion size, burr, and blood flow. Sonographer BI-RADS grading is a classification of BI-RADS that is analyzed by sonographers. AI-BI-RADS grading indicates the BI-RADS classification obtained by AI software based on AI risk score analysis.

or malignant lesions, with complex and diverse imaging findings.[14,15] Especially when the ultrasound image is complicated with other lesions. To improve the diagnostic accuracy of this disease, some scholars have done relevant studies. Liu et al[16] analyzed the ultrasonic characteristics and elastic information of 347 cases of invasive ductal carcinoma and 54 cases of simple SA and concluded that calcification and vascular distribution could be used as independent indicators for differential diagnosis, and elastic imaging could be a powerful tool to assist the diagnosis of SA. Liang et al[17] established a nomogram to distinguish nodular SA from malignant tumors based on clinical data and ultrasonic characteristics and believed that the nomogram could be used as a supplementary means to accurately distinguish breast lesions that needed biopsy. However, there are differences in the resolution of different machines and the interpretation standards and methods of images by researchers, which are susceptible to subjective analysis and biases. Radiomics has been recognized by scholars in the study of breast lesions because it is not affected by human factors and can carry out an objective analysis of gray-scale images. Huang et al[18] applied radiomic texture analysis technology and combined three variables, radiomic score, BI-RADS, and palpable mass, as independent influencing factors for modeling. They believe that the model developed based on radiomics, ultrasound features, and clinical manifestations can be used as a potential candidate diagnostic tool to distinguish SA from IDC, which can help in clinical diagnosis.[18] They believe that the model developed based on radiomics, ultrasound features, and clinical manifestations can be used as a potential candidate diagnostic tool to distinguish SA from IDC, which can help in clinical diagnosis.[18] However, the process of radiomic feature analysis is complicated, which requires access to standard images, import into specific software, and then manually tracing and analyzing the gray-scale image texture.

In this study, an AI-assisted breast diagnosis system and two-dimensional ultrasound were used for synchronous examination, which was convenient and fast. The system quantified the grayscale characteristics of masses through deep learning of lesion information, and gave classification and risk scores more objectively and scientifically, thus reducing the subjective influence of the observer and achieving report homogeneity. The study found that AI risk score could be used as an independent risk factor and was incorporated into the prediction model. As a quantitative indicator, the AI risk score reflected the malignant degree of lesions. The AI risk scores of SA and IBC in the training group were 0.42±0.26 and 0.78±0.12, respectively. At the same time, the combination of patient age, lesion size, burrs, and blood supply in ultrasound characteristics can greatly improve the risk prediction.

In this study, for the first time, a stratified analysis of lesion size was performed to exclude larger tumors and select early breast cancer patients with no lymph node metastasis at the T1 stage. In the training group, the maximum lesion diameter of SA and IBC was 11mm (8.00; 14.75) and 14.00 mm (12.00; 17.00), which was statistically significant. In tumors smaller than 2 cm, we found that lesion size was still an independent predictor for distinguishing SA and IBC, indicating that SA was smaller than malignant lesions, which was consistent with previous studies.[19] This also suggests that in clinical work, attention should be paid to small lesions in the identification of the two, especially in premenopausal women. Previous studies believed that SA was the most common in women aged 45–55.[1,20] We found that in the training group, the median age of SA patients was 44 years, which was younger than that of patients with early breast cancer (median age 49 years); thus, the identification of SA and IBC is most clinically valuable and significant in women with lesions less than 2 cm in diameter and aged 40–50 years. The study found that there were no burrs at the edge of the ultrasound features, and the blood supply was also an independent predictor. The structure of the lobule was distorted due to the combination of interstitial hyperplasia and increased fiber

components of SA, and some nodules showed irregular burr changes at the edge in imaging. Among the 110 SA patients in the training group, 39 cases (35.45%) showed burr changes at the lesion edge, but their AI risk score was lower than that of IBC patients. It may be due to that it is different from the pathological mechanism of the burr sign of malignant lesions,[21] and it is difficult to observe subtle changes with the naked eye, but artificial intelligence can identify anomalies through grayscale analysis. Therefore, the AI risk score plays a potential role in identifying these lesions with burr signs. SA lesions are mostly characterized by no blood supply or lack of blood supply, and breast cancer shows a short strip blood flow signal or richer blood flow state at the early stage, which is directly related to malignant lesions accompanied by neovascularization. Therefore, when examining small nodules, the technique should be gentle and the machine parameters should be pre-adjusted to show the real blood flow situation of the lesion and surrounding tissues.

In determining the indicators to be included in logical analysis and nomogram construction, in addition to the ultrasonic indicators such as lesion size, two-dimensional gray scale characteristics, and lesion blood flow, the significance of patient age and AI risk score in the differentiation of the two diseases should also be considered. Our combined model better combines ultrasound diagnosis with AI information, and can be used as a supplement to BI-RADS classification for clinical diagnosis.

Our study is a retrospective analysis, and there are still some limitations: Firstly, this study did not compare and observe the consistency between doctors with different seniority and AI-assisted systems, and whether observers with different experiences would be affected by subjective experience. Secondly, the disease types were not detailed. SA is often complicated with benign and malignant lesions such as fibroadenoma and intraductal papilloma. In our statistical sample, 28 cases of SA complicated with malignant lesions were excluded, and most of these cases were complicated with ductal carcinoma in situ (20/28). SA itself is caused by interstitial hyperplasia leading to the distortion of lobular acinar structure; thus, it is still unclear whether interstitial fibrosis increases the risk of cancer or not.[22] Due to the limited number of cases, we will continue to accumulate sample size in the future, and predict the future risk of cancer in SA through the analysis of molecular expression status[23] and other relevant characteristics. Nomogram is widely used in the medical field to predict disease prognosis and medical event outcomes by combining multiple risk factors.[24] The study found that clinical ultrasonic-AI combined nomogram has good diagnostic performance. The establishment of this model not only provides a more effective diagnostic tool for clinicians but also contributes to the stratified risk management of SA patients in the future. Although ultrasound doctors have certain subjectivity and differences in image interpretation standards and methods, at this stage, the development of AI cannot completely replace ultrasound doctors. Therefore, the combination of ultrasound doctors and AI-assisted systems will be the general trend in the development of ultrasound medicine in the future.

Data Sharing Statement

The datasets used and/or analyzed during the current study are available from the corresponding author on reasonable request.

Study Approval Statement

This study conformed to the ethical guidelines of the Declaration of Helsinki as reflected in a priori approval by the human research committee of Henan Provincial People's Hospital.

Consent to Participate Statement

The written informed consent was acquired from each patient.

Funding

There is no funding to report.

Disclosure

The authors declare that they have no competing interests for this work.

References

1. Visscher DW, Nasser A, Degnim AC, et al. Sclerosing adenosis and risk of breast cancer. *Breast Cancer Res Treat*. 2014;144(1):205–212. doi:10.1007/s10549-014-2862-5
2. Yoshida A, Hayashi N, Akiyama F, et al. Ductal carcinoma in situ that involves sclerosing adenosis: high frequency of bilateral breast cancer occurrence. *Clin Breast Cancer*. 2012;12(6):398–403. doi:10.1016/j.clbc.2012.08.002
3. Chen YL, Chen JJ, Chang C, et al. Sclerosing adenosis: ultrasonographic and mammographic findings and correlation with histopathology. *Mol Clin Oncol*. 2017;6(2):157–162. doi:10.3892/mco.2016.1108
4. Guirguis MS, Adrada B, Santiago L, Candelaria R, Arribas E. Mimickers of breast Malignancy: imaging findings, pathologic concordance and clinical management. *Insights Imaging*. 2021;12(1):53. doi:10.1186/s13244-021-00991-x
5. Huang N, Chen J, Xue J, et al. Breast sclerosing adenosis and accompanying Malignancies: a clinicopathological and imaging study in a Chinese population. *Medicine*. 2015;94(49):e2298. doi:10.1097/md.0000000000002298
6. Bacci J, MacGrogan G, Alran L, Labrot-Hurtevent G. Management of radial scars/complex sclerosing lesions of the breast diagnosed on vacuum-assisted large-core biopsy: is surgery always necessary? *Histopathol*. 2019;75:900–915. doi:10.1111/his.13950)
7. Leibig C, Brehmer M, Bunk S, et al. Combining the strengths of radiologists and AI for breast cancer screening: a retrospective analysis. *Lancet Digit Health*. 2022;4(7):e507–e519. doi:10.1016/S2589-7500(22)00070-X
8. Pfob A, Sidey-Gibbons C, Barr RG, et al. The importance of multi-modal imaging and clinical information for humans and AI-based algorithms to classify breast masses (INSPiRED 003): an international, multicenter analysis. *Eur Radiol*. 2022;32(6):4101–4115. doi:10.1007/s00330-021-08519-z
9. Tan H, Zhang H, Lei Z, Fu F, Wang M. Radiological and clinical findings in sclerosing adenosis of the breast. *Medicine*. 2019;98(39):e17061. doi:10.1097/md.0000000000017061
10. Gradishar WJ, Moran MS, Abraham J, et al. Breast cancer, version 3.2022, NCCN clinical practice guidelines in oncology. *J Natl Compr Cancer Netw*. 2022;20(6):691–722. doi:10.6004/jnccn.2022.0030
11. D'Orsi CJ, Sickles EA, Mendelson EB, Morris EA. *ACR BI-RADS Atlas, Breast Imaging Reporting and Data System*. Reston, VA: American College of Radiology; 2013.
12. Wu GG, Zhou LQ, Xu JW, et al. Artificial intelligence in breast ultrasound. *World J Radiol*. 2019;11(2):19–26. doi:10.4329/wjr.v11.i2.19
13. Shao S, Yao M, Li X, et al. Conventional and contrast-enhanced ultrasound features in sclerosing adenosis and correlation with pathology. *Clin Hemorheol Microcirc*. 2021;77(2):173–181. doi:10.3233/CH-200943
14. Sharma T, Chaurasia JK, Kumar V, et al. Cytological diagnosis of sclerosing adenosis of breast: diagnostic challenges and literature review. *Cytopathology*. 2021;32(6):827–830. doi:10.1111/cyt.13041
15. Ruan M, Ding Z, Shan Y, et al. Radiomics based on DCE-MRI improved diagnostic performance compared to BI-RADS analysis in identifying sclerosing adenosis of the breast. *Front Oncol*. 2022;12:888141. doi:10.3389/fonc.2022.888141
16. Liu W, Li W, Li Z, et al. Ultrasound characteristics of sclerosing adenosis mimicking breast carcinoma. *J Breast Cancer Res Treat*. 2020;181(1):127–134. doi:10.1007/s10549-020-05609-2
17. Liang T, Cong S, Yi Z, et al. Ultrasound-based nomogram for distinguishing malignant tumors from nodular sclerosing adenoses in solid breast lesions. *J Ultrasound Med*. 2021;40:2189–2200. doi:10.1002/jum.15612
18. Huang Q, Nong W, Tang X, et al. An ultrasound-based radiomics model to distinguish between sclerosing adenosis and invasive ductal carcinoma. *Front Oncol*. 2023;13:1090617. doi:10.3389/fonc.2023.1090617
19. Li Y, Wei XL, Pang KK, et al. A comparative study on the features of breast sclerosing adenosis and invasive ductal carcinoma via ultrasound and establishment of a predictive nomogram. *Front Oncol*. 2023;13:1276524. doi:10.3389/fonc.2023.1276524
20. Yu BH, Tang SX, Xu XL, et al. Breast carcinoma in sclerosing adenosis: a clinicopathological and immunophenotypical analysis on 206 lesions. *J Clin Pathol*. 2018;71(6):546–553. doi:10.1136/jclinpath-2017-204751
21. Yamaguchi J, Ohtani H, Nakamura K, et al. Prognostic impact of marginal adipose tissue invasion in ductal carcinoma of the breast. *Am J Clin Pathol*. 2008;130(3):382–388. doi:10.1309/MX6KKA1UNJ1YG8VN
22. Lu P, Weaver VM, Werb Z. The extracellular matrix: a dynamic niche in cancer progression. *J Cell Biol*. 2012;196(4):395–406. doi:10.1083/jcb.201102147
23. Nassar A, Hoskin TL, Stallings-Mann ML, et al. Ki-67 expression in sclerosing adenosis and adjacent normal breast terminal ductal lobular units: a nested case-control study from the Mayo Benign Breast Disease Cohort. *Breast Cancer Res Treat*. 2015;151(1):89–97. doi:10.1007/s10549-015-3370-y
24. Hong ZL, Chen S, Peng XR, Li JW, Yang JC, Wu SS. Nomograms for prediction of breast cancer in breast imaging reporting and data system (Bi-rads) ultrasound category 4 or 5 lesions: a single-center retrospective study based on radiomics features. *Front Oncol*. 2022;12:894476. doi:10.3389/fonc.2022.894476